REINFORCEMENT-FREE DECKS USING A MODIFIED STRUT-AND-TIE MODEL

Han Ug Bae, Michael G. Oliva, Lawrence C. Bank

Department of Civil and Environmental Engineering, University of Wisconsin-Madison, 2205 Engineering Hall, 1415 Engineering Drive, Madison, WI 53706.

Biography: Han Ug Bae is a postdoctoral fellow in Civil and Environmental Engineering at University of Wisconsin-Madison. He received his BS and MS from Yonsei University, Seoul, Korea and PhD from University of Wisconsin-Madison. His research interests include strut-and-tie models, development of highway bridge design methods and bridge construction.

Michael G. Oliva is a Professor in the Department of Civil and Environmental Engineering at University of Wisconsin-Madison. He received his BS from University of Wisconsin-Madison; MS and PhD from University of California, Berkeley. His research interests include highway bridges, reinforced-precast-prestressed concrete design and earthquake resistance.

ACI member **Lawrence C. Bank** is a Professor in the Department of Civil and Environmental Engineering at University of Wisconsin-Madison. He received his BS from Technion- Israel Institute of Technology, Haifa, Israel; MS and PhD from Columbia University. He is a member of ACI committee 440 (Fiber Reinforced Polymer Reinforcement). His research interests include FRP composites in structural engineering, mechanics of composite materials and innovative bridge construction.

ABSTRACT

This paper describes an application of a modified strut-and-tie model (STM) for determining the strength of reinforcement-free bridge decks on concrete wide flange girders. The method could also be applied to other short span restrained concrete slabs. The concept presented for the reinforcement-free bridge deck includes a combination of removing steel reinforcement, utilizing

compressive membrane action in the deck by tying girders together, and introducing a polypropylene fiber to control shrinkage cracks. An analysis method for these reinforcement-free decks using a modified STM that considers geometrical nonlinearity is proposed. The model provides a 2D axisymmetric representation of the behavior of the reinforcement-free deck and it is capable of capturing punching and flexural failure. Comparisons to nonlinear FEM analysis results were made to verify the proposed analysis method. A design load appropriate for reinforcement-free bridge decks is proposed.

Keywords: strut-and-tie model; reinforcement-free deck; punching shear; precast prestressed girder; bridge decks; compressive membrane action; deck analysis; and wide flange concrete girder.

INTRODUCTION

The strut-and-tie model (STM) developed by Schlaich et al.[1] is considered to be a powerful new model for design and analysis of disturbed or discontinuous regions (D-regions) where geometrical or structural complexity exists in concrete members. The model is recognized in ACI 318[2] and numerous investigations and modifications of the method have been performed.[3-6]

The STM can be used for a restrained short span bridge deck on girders since the deck behaves like a D-region. Concentrated forces develop where the girder supports the deck and at the center of the span under a wheel load. Compressive membrane action (CMA) develops in the restrained deck and changes the failure mode from a flexural failure to a punching shear failure, enhancing the capacity, if sufficient lateral restraint is provided.[7] Lateral restraint in the deck around the loaded region inhibits rotation, which is accompanied by translation in the plane of the deck, and leads to an enhancement of the flexural capacity of the deck. Analysis methods to predict the enhanced capacity of the restrained deck have been suggested by a number of researchers.[8,9] These methods only consider the punching failure mode, but flexural failure can also occur if there is insufficient lateral restraint.

One application of CMA has been in steel-free bridge decks in Canada.[10,11] Another application of CMA for decks has been in a bridge using a reinforcement-free deck on concrete wide flange girders that was built in Wisconsin.[12] Considering the development of a strut system in the restrained deck showed that conventional flexural steel reinforcement deck could be eliminated. The mechanism considers CMA in the deck obtained by the natural high lateral stiffness of wide flanged precast concrete girders with special ties between girders provided by steel rods through their webs (**Fig. 1**). Polypropylene fiber, at a volume fraction of 0.32 %, was added to the concrete mix to help control early plastic shrinkage.[13] Laboratory experiments[14] indicated that the deck had sufficient service and ultimate capacities to resist vehicular loads, without flexural reinforcing, leading to construction of the prototype bridge on a U.S. Highway.[12]

In this paper, a modified STM is developed to predict the strength of this type of reinforcement-free bridge deck. The existing methods of STM analysis described by ACI 318[2] cannot be used directly to analyze this restrained deck since the punching shear failure behavior of the deck occurs in 3 dimensions and the existing methods cannot capture the enhancement of the flexural strength as a function of the degree of restraint provided.

For special permit trucks, unlike the AASHTO design truck, the wheel loadings may have a different effect on a deck. A strength check (low cycle short term behavior) is, however, possible using the proposed STM without any modification (except for the calculation of the effective flexural strip width of the deck; longitudinal wheel spacing should be used when the spacing is less than the effective width) if the spacings of the wheels are not narrower than the clear deck span.

RESEARCH SIGNIFICANCE

A new method to predict the strength of reinforcement-free bridge decks is presented. Traditional bridge deck analysis and design is based on flexural failure. Since most bridge decks actually fail in punching shear under heavy wheel loading, it is evident that improved strength estimations are needed. The proposed method is capable of capturing punching or flexural failure of the restrained bridge deck between girders while previously developed analytical models only capture one of the failure modes. This new model is a practical and effective method to replace time consuming FEM analysis.

CURRENT DECK DESIGN STRENGTH

The American Association of State Highway and Transportation Officials (AASHTO)[15] provides guidelines for designing or calculating the strength of bridge decks based on the deck flexural resistance between supporting girders. Tests of decks[7,11,14,16,17] have shown that failure actually occurs with punching under wheels at loads of approximately five times the AASHTO design service wheel load (with impact).

Coincidentally research on fatigue of concrete decks using moving loads has found that failure can occur after 100 million cycles of load at values as low as 14% of the static ultimate capacity of the deck.[18] In other words, if the deck is expected to resist 100 million cycles of moving wheel load the design static capacity should be 700% of the fatigue wheel load. The AASHTO fatigue wheel live load, including dynamic load allowance (15 %) and a fatigue load factor (0.75), is 13.8 kips (61.4 kN)[15]. The fatigue design load would then be equal to 97 kips (431 kN). This is also approximately five times the service wheel load – or the capacity now being achieved with a flexural design approach. The fatigue design load is a governing design load since the AASHTO design strength load used in flexural design, including load factor (1.75), dynamic load allowance (33%) and multiple presence factor (1.2) from AASHTO LRFD[15], is 44.7 kips (198.8 kN). To achieve the same fatigue life as attained with the current AASHTO flexural design, the capacity of a deck calculated using the modified STM estimate method described here is regarded as sufficient if it can resist a 97 kip (431 kN) vehicle wheel load.

DESCRIPTION OF MODIFIED STM FOR RESTRAINED CONCRETE DECKS

The modified STM proposed here for predicting bridge deck strength differs from standard STM in that it provides a 2D axisymmetric representation of the behavior of a restrained 3-D bridge deck and in that it is analyzed using 2nd order methods to include geometric nonlinearity of the deck behavior. A detailed description of the proposed model is provided here.

Geometrical configuration of the model

To solve the model in an axisymmetric configuration, the rectangular loaded area from a vehicle wheel is transformed to an equivalent circle, having diameter *D*, with the same area[9] as the actual wheel contact area - shown in Equation (1).

$$D = \sqrt{\frac{4bd}{\pi}} \tag{1}$$

This is acceptable since the punching failure of bridge decks generally occurs with a cone shaped failure surface as shown in **Fig. 2**, even though the loaded area is close to rectangular.[9]

The STM shown in **Fig. 3** is constructed assuming that flexural cracking at the negative moment region near the girder has already developed. The compressive and tensile stress trajectories at the failure load level (visible as discrete lines) predicted by a FEM analysis along section A-A of **Fig. 2** are shown in **Fig. 3** and lead to the suggested STM superimposed over the stress lines. The solid lines of the STM represent struts in compression and the dotted lines represent ties (across the struts) in tension. A spring in the lateral direction is placed at the left and right bottom sides of the model, at the deck supports, to simulate axial restraint from adjoining structural elements.

The model shown in **Fig. 3** is based on an assumption that that the punching failure surface reaches the edge of the girder. From the results of FEM deck modeling, this assumption appears valid for restrained decks thicker than 7 in. (178 mm) with clear deck spans less than 5 ft. (1524 mm). This limitation does not hinder the practical application of the modified STM since the minimum thickness deck prescribed in the AASHTO LRFD bridge design specification[15] is 7 in. (178 mm) and the clear deck span in a bridge with wide flange concrete girders rarely exceeds 5 ft. (1524 mm).

It is possible to replace the detailed modeling of the diagonal struts shown in **Fig. 4(b)** with a single diagonal strut as shown in **Fig. 4(a)** as will be described later. The single diagonal strut represents a half portion of the failure surface in **Fig. 2(c).** The stiffness of the springs at each side of the 2D STM represent the radial outward stiffness caused by restraint from the adjoining slab over a half of the failure line at the bottom fiber shown in **Fig. 2(a)**.

Locations for the top and bottom ends of the diagonal strut were determined using a linear bending stress distribution and are shown in **Fig. 4(a)**. The vertical locations of the top lateral strut and the bottom end of the diagonal strut were assumed at the resultants of triangular compressive stress distributions at mid-span where positive moment occurs and near the girder where negative moment occurs, respectively. These placements coincided well with the center of gravity of the compressive stress distribution at these locations predicted from a nonlinear FEM analysis close to the failure load level.

The length of the diagonal strut, l_{ds}, and the angle of inclination of the diagonal strut, θ_1, can be calculated using the dimensions from **Figs. 2** and **4**. The average width of the diagonal strut, w_{ds}, that represents the 3-D circumferential surface in the *r* direction shown in **Fig. 4(a)** can be calculated as the average of the top and the bottom half circumference of the cone of **Fig. 2**.

$$w_{ds} = \frac{\pi}{4}\left(\frac{D}{2} + L\right) \tag{2}$$

It is also necessary to find the width of the diagonal strut for the model in x-y plane (w_{avg}) in **Fig. 4(a)**. The width of the diagonal strut at its bottom and its top can be calculated as,

$$w_1 = \frac{t}{3}\cos\theta_1, \quad w_2 = \frac{D}{2}\sin\theta_1 + \frac{t}{3}\cos\theta_1 \tag{3}$$

An average width of the diagonal strut (w_{avg}) is taken as the average of the average width of the widths at the two ends and the maximum width of the bottle shaped strut (w_3) as shown in Equation (4). The maximum width (w_3) of the actual bottle shaped strut shown in **Fig. 4(a)** must be found from the compressive stress field using a FEM analysis. This analysis has already been completed[14] for decks on bridges with wide flange concrete girders and the values for w_3 can be calculated using

Table 1.

$$w_{avg} = \frac{1}{2}(\frac{w_1 + w_2}{2} + w_3) \quad (4)$$

The average cross-sectional area of the diagonal strut can then be calculated as,

$$A_{ds} = w_{avg} w_{ds} \quad (5)$$

Stiffness of the spring in the model

The stiffness of the lateral spring at the supports in the model is a combination of the lateral tie stiffness, the bending stiffness of the girder about its weak axis, the torsional stiffness of the girder, and the in-plane stiffness of the adjoining slab. These components behave like springs in series as shown in **Fig. 5** since the deck is restrained by the girders and the girders are restrained by the ties. To be conservative, spring stiffness was just calculated for a deck span adjacent to an external girder since the lowest lateral restraint occurs at this location. A diagram used to calculate the stiffness of the springs on the exterior side of the 2D STM is shown in **Fig. 6.** Two approximations are made here: 1) around one half of the bottom of the conical failure surface the restraint is taken as similar to that on the side toward the exterior girder and 2) around the other half the adjacent deck material is assumed to be rigid. The first assumption is judged to be conservative and it appears to be reasonable since the shear failure will start at the location nearest to the exterior girder and then propagate circumferentially. This was found from the observation of the nonlinear FEM analysis, though difficult to see in actual load testing because of the rapid crack growth. The second assumption is made since that side is restrained by a relatively rigid large deck acting as a flat horizontal diaphragm as shown in **Fig. 5**.

The displacement δ_l in **Fig. 6** represents the lateral displacement at the bottom left of the exterior strut due to a combination of elongation of the tie, lateral flexural displacement of the girder and torsional rotation of the girder. These deformations are caused by a vertical force which induces a unit distributed load q in the radial direction in the 3D model. The sum of radial outward thrust in the form of a single force in the 2D model can be calculated as,

$$P_l = q \times \frac{\pi}{2} L \tag{6}$$

The stiffness of the spring at the bottom left side of the 2D model would be given by Equation (7) using Equation (6) if δ_l were known.

$$K_l = \frac{P_l}{\delta_l} = \frac{q\pi L}{2\delta_l} \tag{7}$$

Tension tie contribution to spring stiffness:

The lateral stiffness provided by the tension ties, K_{tt}, in resisting a single vehicle wheel can be calculated from Equation (8) assuming that the girder is rigid. The tension ties for a particular deck span are anchored on the opposite sides of the girder webs. The length is then S_g, the girder spacing plus the web thickness t_w. If the spacing of ties is S_t, spacing of vehicle axles is S_w, and tie area is A_t then the stiffness is given as,

$$K_{tt} = \frac{A_t E_s}{S_t (S_g + t_w)} S_w \tag{8}$$

The total transverse lateral force resisted by the ties, due to a single vehicle wheel load, can be calculated as the clear span of the deck (L) times the unit distributed load (q) as shown in **Fig. 7**. The lateral displacement δ_l due to the elongation of the ties alone can be calculated from the total force divided by the lateral stiffness of the tension ties as,

$$\delta_{lt} = \frac{L \times q}{K_{tt}} = \frac{L S_t (S_g + t_w) q}{A_t E_s S_w} \tag{9}$$

The stiffness of the spring at the bottom left side of the 2D model, K_{lt}, as contributed by the lateral tension ties is found using Equations (7) and (9) as,

$$K_{lt} = \frac{q\pi L}{2\delta_{lt}} = \frac{\pi A_t E_s}{2 S_t (S_g + t_w)} S_w \tag{10}$$

Girder bending contribution to spring stiffness:

The lateral displacement of the girder due to the lateral weak axis bending , δ_{lgb}, when the patch loads are acting as shown in **Fig. 7,** are calculated by assuming the girder to be supported by the tension ties, i.e. there is no lateral displacement at the tie locations. The girder is conservatively taken as simply supported laterally at the two adjacent ties nearest to the wheel patch load. If I_{yg} is the lateral girder moment of inertia then the added lateral displacement is given as

$$\delta_{lgb} = \frac{qL\left(S_t^{\,3} - \frac{L^2}{2}S_t + \frac{L^3}{8}\right)}{48E_g I_{yg}} \tag{11}$$

The stiffness of the spring at the bottom left side of the 2D model, due to the weak axis bending of the girder, can be calculated by using Equations (7) and (11) as,

$$K_{lgb} = \frac{q\pi L}{2\delta_{lgb}} = \frac{24\pi E_g I_{yg}}{S_t^{\,3} - \frac{L^2}{2}S_t + \frac{L^3}{8}} \tag{12}$$

Girder torsional contribution to spring stiffness:

Additional lateral displacement of the deck occurs due to girder torsion. This needs to be found by a separate analysis for the full length of the girder, applying the unit distributed load q from a single wheel over the length L as shown in **Fig. 8(a)**. The torsional deformations of the ends of the girder near the abutment or pier are assumed to be fixed since concrete diaphragms are generally used at these locations. The analytical model of **Fig. 8(a)** must include the ties and their stiffnesses as well as the girder properties to properly model the restraints on girder deformation. The ties are assumed fixed at their opposite ends. The lateral displacement (δ_1) shown in **Fig. 8(b)** from the analysis includes the displacement from the elongation of the ties, the weak axis bending of the girder and the torsional displacement. The torsional portion of the displacement can be found as,

$$\delta_{lgt} = \delta_1 - \delta_2 \tag{13}$$

This analysis has already been conducted[14] for typical wide flange bulb-tee bridge girders between

54 and 72 in. (1370 to 1830mm) deep and the values for δ_{lgt} are given in **Table 2**.

The stiffness of the spring at the bottom left side of the 2D model due to torsion of the girder can be calculated as,

$$K_{lgt} = \frac{q\pi L}{2\delta_{lgt}} \tag{14}$$

The combined stiffness of the springs in series at the bottom left side of the 2D model in **Fig. 6** can be calculated using the individual stiffnesses from Equations (10), (12) and (15) as,

$$\frac{1}{K_{lm}} = \frac{1}{K_{lt}} + \frac{1}{K_{lgb}} + \frac{1}{K_{lgt}} \tag{15}$$

Capacity of the diagonal strut

The sum of the tensile forces (T) developed in the ties of the detailed diagonal strut in **Fig. 4(b)** when punching failure occurs can be calculated from Equation (16) with the maximum compression force applied to the diagonal strut. The spreading angle (θ_2) can be found from the compressive stress trajectories using a FEM analysis as shown in **Fig. 3.** This has already been completed[14] for typical deck spans on wide flanged concrete girders and the values for θ_2 are given in **Table 3.**

$$T = P_{usd} \tan\left(\frac{\theta_2}{2}\right) \tag{16}$$

Punching failure of the deck occurs when the ties in **Fig. 4(b)** reach the tension capacity of the deck concrete. The sum of the resisting tensile strength capacity across a strut in the model can be calculated by assuming that it is equal to the concrete tensile strength (f_{ct}) over the area of the inclined crack of the conical failure surface adjusted by a crack length ratio (R_1) as given in Equation (17). The crack length ratio is defined as the length of crack along the diagonal strut over the length of the strut. The cracked length was found from FEM analyses of the portion of the compressive strut where the strain in a perpendicular direction to the strut becomes plastic at failure. This analysis has also been completed[14] and values for R_1 for decks on wide flange concrete girders are given in **Table 4.**

$$T_r = f_{ct} R_1 l_{ds} w_{ds} \tag{17}$$

The axial capacity of the diagonal strut, when diagonal cracking and tension failure (punching failure) develops, can be calculated from Equation (18) by equating Equations (16) and (17).

$$P_{uds} = \frac{f_{ct} R_1 l_{ds} w_{ds}}{\tan\left(\frac{\theta_2}{2}\right)} \tag{18}$$

Capacity of the top strut

The capacity of the top lateral strut in the STM in **Fig. 4(a)** can represent flexural failure of the deck due to crushing of the concrete. This capacity can be calculated by flexural analysis of a rectangular reinforced concrete section with tension reinforcement only (**Fig. 9**). The width of concrete resisting the compression is assumed to be the effective flexural strip width of the deck as given in AASHTO LRFD (2008) Table 4.6.2.1.3-1[15] as $E_w = 26+6.6S_g$ (SI units: $E_w = 660.4+0.55S$) where E_w = distribution width [in. (mm)], and S_g = center to center spacing of the girders [ft. (mm)].

The cross section of the tension reinforcement can be obtained by converting the lateral stiffness to steel reinforcement with identical stiffness. The tension reinforcement is actually a “virtual” concept since the lateral thrust (restraint) applied at the outside of the struts actually balances the top compression force and the virtual tension reinforcement represents the lateral thrust. Assume that the virtual reinforcement does not yield at the ultimate state. In a wide range of deck studies completed[14], the overall lateral restraint system (adjacent deck, beam lateral and torsional stiffnesses, and ties) remained elastic. The lateral stiffness value calculated in Equation (15), however, is the stiffness in the radial direction for half the circular cone failure surface and it is necessary to convert to the stiffness in the lateral direction only. The lateral stiffness portion of the combined lateral stiffness over the distribution width (E_w) can be calculated as,

$$K_{lf} = K_{lm} \frac{2}{\pi} \frac{E_w}{L} \tag{19}$$

The cross-sectional area of the virtual steel reinforcement (A_{vr}) can be calculated from,

$$K_{lf} = \frac{A_{vr} E_s}{L} \tag{20}$$

The compressive force (C) in the compression block and the tensile force (T) in the virtual reinforcement when the flexural failure occurs are shown in Equation (21) if a is the compression block depth and ε_{vr} is the strain in the virtual reinforcement (**Fig. 9**).

$$C = 0.85 f_c' E_w a \,, \quad T = A_{vr} E_s \varepsilon_{vr} \,, \quad C = T \tag{21}$$

The strain compatibility at the ultimate state shown in **Fig. 9** gives Equation (22).

$$0.003 \frac{5}{6} t = (0.003 + \varepsilon_{vr}) \frac{a}{\beta_1} \tag{22}$$

a and ε_{vr} can be found using Equations (21) and (22). The capacity "C" of the lateral top strut can then be found by using the calculated a and Equation (21) as,

$$P_{utls} = 0.85 f_c' E_w a \tag{23}$$

Creating a Stable STM

The final step in the use of the new model is to perform a 2nd order analysis (large displacement). 2nd order analysis is necessary because the resistance and stability of the model are dependent on the lateral displacements at the bottom joints. As shown in **Fig. 4(a)**, however, the model is not currently a proper truss because of the lack of triangulation and equivalent model is assumed without a horizontal top lateral strut as shown in **Fig. 10**. The lateral spring at the left side is replaced with a bottom "virtual" tie or reinforcing having the identical restraining stiffness. The failure of the deleted top lateral strut is duplicated by assigning the bottom lateral tie an identical failure capacity since the axial force in the top and bottom members would be identical.

VERIFICATION OF STM CAPACITY PREDICTIONS

Since extensive deck tests are expensive and inefficient, the accuracy of nonlinear FEM analysis strength prediction for a large series of deck configurations was used as a basis of comparison with the STM strength predictions. ABAQUS[19] was used to conduct the FEM analyses. A complete description of the FEM analysis technique is provided elsewhere[14, 20]. Validation of the FEM analysis method strength prediction capability was achieved by comparison with a restrained deck element experimental test as shown in **Fig. 11**. [14, 20] The strength prediction error was 6%, an acceptable amount for estimating capacity of a structure that is very non-linear with a non-homogenous material.

A parametric study on the ultimate capacity of bridge decks using both FEM analysis and the modified STM were performed to verify the STM predictions and to identify key performance characteristics affected by design parameters. Ninety four analyses were conducted with variations in deck depth, span, concrete strength, girder type and size, and restraint provided by ties between Wisconsin 54 inch (1372 mm) deep girders[21].

A deck restraing factor "*R*" given in Equation (24) was derived to describe the restraint provided by steel ties between the girders.

$$R = \frac{(axial\ stiffness\ of\ a\ lateral\ steel\ tie) \times (thickness\ of\ deck)}{(center\ to\ center\ spacing\ of\ girders) \times (spacing\ of\ lateral\ steel\ ties)} \tag{24}$$

The results for a 7.5 in. (191 mm) deep deck with a 6 ft. (1829 mm) lateral tie spacing are shown in **Fig. 12**. The comparison of the FEM and STM methods shows generally acceptable agreement, i.e. small error, for clear deck spans less than 6 ft. (1830mm). When the clear deck span was 6 ft. (1830 mm) the STM analysis showed 4 ~ 18 % higher capacity compared to the FEM analysis. These results indicate the STM may be unsafe for long span deck capacity and the application should be limited to normal deck spans.

The failure mode changes from flexural to punching shear if an appropriate level of restraint exists. The required amount of restraint appears to depend on the deck span length. Shear failure generally occurred when the restraint (R) was above 600 lb/in^2 (4.13 N/mm^2). Improvement in the ultimate strength is minimal with an increase of the deck restraining factor (R) over 900 lb/in^2 (6.20

N/mm^2). It is, therefore, recommended to design the lateral steel tie to provide the deck with a restraining factor (R) of at least 900 lb/in^2 (6.20 N/mm^2).

FEM and STM analyses for a 7.5 in. (191 mm) deep deck with 8 ft. and 10ft. (2438 mm or 3050 mm) lateral tie spacings were also performed. The results were similar to those shown in **Fig. 12.** The results indicate that for a given span length, deck thickness and deck restraining factor, the failure capacity does not change significantly with tie spacings between 6ft. and 10ft. (1830 mm and 3050 mm). Additional FEM and STM analyses were performed for two other types of wide flange girders, Wisconsin 72W girders and Washington state WS53 girders, and the comparison showed generally acceptable agreement[14, 20].

SIMPLIFIED CAPACITY EQUATION

An alternate simpler method to predict the ultimate capacity of reinforcement-free decks on 54 to 72 in. (1372 to 1829 mm) deep wide flanged precast girders, for a wheel having an AASHTO[15] patch size, is given by P_d as,

$$P_d = 13 t_d^{\,1.894} L_d^{\,-0.541} \left(\frac{K_{td}}{S_{td}}\right)^{0.225} \qquad \left(\text{SI units: } P_d = 2.227 t_d^{\,1.894} L_d^{\,-0.541} \left(\frac{K_{td}}{S_{td}}\right)^{0.225}\right) \qquad (25)$$

The equation was fitted to results from the FEM parametric analyses. Restraint factors (R) of 200 lb/in^2 to 1200 lb/in^2 (1.38 N/mm^2 to 8.27 N/mm^2) were used with clear spans of 3 ft to 6 ft. (914 mm to 1829 mm), deck thicknesses of 7.0 in. to 9.0 in. (178 mm to 229mm) deck thickness, and lateral steel tie spacing of 6 ft. to 10 ft. (1829 mm to 3048 mm).

The equation on average predicted 94.8 % of the deck capacity defined by FEM analysis results. The standard deviation was 5.8 %. The relationship between the predicted capacities of the deck using the proposed equation and those of the deck using nonlinear FEM analysis is shown in **Fig. 13**. The bold line in **Fig. 13** indicates the result if the two analyses matched perfectly. Most of the points are at the upper side of the bold line indicating that the proposed equation is conservative.

STM CAPACITY CALCULATION EXAMPLE

A step by step capacity calculation example for a reinforcement-free deck on 54 in. (1372mm) deep wide flanged girders using the developed equations and the alternative equation is illustrated here.

1) Given information for the sample deck on Wisconsin 54W girders when the clear span of the deck between girders is known:

Clear span of the deck:	L = 4ft. (1219 mm)
Spacing of the girders:	S_g = 8ft. (2438 mm)
Thickness of the web of the girder:	t_w = 6.5 in. (165 mm)
Design compressive strength of the deck:	f_c' = 4000 psi (27.6 MPa), β_1 =0.85
Design compressive strength of the girder:	f_c' = 8000 psi (55.1 MPa)
Modulus of elasticity of the deck:	E_d = 3605 ksi (24.8 GPa)
Modulus of elasticity of the girder:	E_g = 5098 ksi (35.1 GPa)
Moment of inertia of the girder in weak axis:	I_{yg} = 125056 in.^{4} ($52{,}052 \times 10^6$ mm^4)
Modulus of elasticity of the lateral steel tie:	E_s = 29,000 ksi (199.8 GPa)
Spacing of the vehicle axles in longitudinal direction:	S_w = 14 ft. (4267 mm)
Depth of the deck:	t = 7.5 in. (191 mm)
Spacing of lateral steel ties:	S_t = 10 ft. (3048 mm)

2) Find the needed axial stiffness of a single lateral tie (K_t) from Equation (24) using the recommended deck restraining factor (R) = 900 lb/in^2. (6.20 N/mm^2)

$$K_t = (900 \text{ lb/in}^2)\, S_g\, S_t / t = 1382.4 \text{ kip/in (242.1 kN/mm)}$$

3) Calculate the cross-sectional area of a single lateral tie from the axial stiffness found above.

$$K_t = \frac{A_t E_s}{(S_g + t_w)}, \quad A_t = \frac{K_t (S_g + t_w)}{E_s} = 4.886 \text{ in.}^2 \text{ (3152 mm}^2\text{)}$$

Assume tension tie bars with 2.5 in. (64 mm) diameter.

$$A_t = \frac{\pi (2.7in)^2}{4} = 4.909 \text{ in.}^2 \text{ (3167 mm}^2\text{)}$$

4) Find parameters from **Tables 1-4.**

$$\theta_2 = 53.117°,\ R_2 = 1.50,\ R_1 = 0.565,\ \delta_{\lg t} = 0.0257 \text{ in. } (0.653 \text{ mm})$$

5) Predict the ultimate capacity of the deck system using the modified STM analysis.

Calculate cross-sectional area of the diagonal strut using Equations (1)-(5).

θ_1 =14.03°, l_{ds} = 20.63 in. (524.00 mm), D = 15.96 in. (405.38 mm), w_{ds} = 43.97 in. (1116.73 mm),

w_1 = 2.43 in. (61.61 mm), w_2 = 4.36 in. (110.73 mm), w_{avg} = 6.79 in. (172.34 mm),

$$A_{ds} = 298.31 \text{ in.}^2\ (192{,}457.40 \text{ mm}^2)$$

Calculate combined restraint K_{lm} using Equations (10), (12), (13) and (15)

$$K_{lt} = 3{,}054{,}324 \text{ lb/in. } (534{,}867 \text{ N/mm}),\ K_{\lg b} = 29{,}977{,}388 \text{ lb/in. } (5{,}249{,}583 \text{ N/mm})$$

$$K_{\lg t} = 2{,}933{,}783 \text{ lb/in } (513{,}759 \text{ N/mm}),\ K_{lm} = 1{,}425{,}273 \text{ lb/in. } (249{,}591 \text{ N/mm})$$

Calculate capacity of the truss members using Equations (18)-(23)

P_{uds} = 324,087 lb (1,441,541 N), $E_w = 26 + 6.6S$ = 78.8 in. (2001 mm), A_{vr} = 2.446 in.^{2} (mm^2),

$$a = 1.701 \text{ in. } (43.21 \text{ mm}),\ P_{utls} = 455{,}604 \text{ lb } (2{,}026{,}527 \text{ N})$$

Construct the modified STM and perform 2nd order (P-delta) analysis to check if the model has sufficient capacity to withstand the design load [97 kips (431 kN)].

The member forces of the model under the design load were 218.4 kips (971 kN) for the diagonal member and 231.6 kips (1030 kN) for the lateral member, indicating that the section of the deck system is safe.

The ultimate capacity found from the second order truss analysis was 141.3 kips (629 kN). The member forces at the failure of the model were 324.1 kips (1442 kN) for the diagonal member and 318.0 kips (1414 kN) for the lateral member. The diagonal member reached its capacity first - indicating that the failure mode was a punching failure.

6) Comparison with the result using the proposed equation alternative to the modified STM analysis.

Use Equation (25) to calculate the predicted capacity of the deck.

t_d = 7.5 in. (191 mm), L_d = 4ft. = 48 in. (1219 mm),

$$K_{td} = \frac{A_t E_s}{(S_g + t_w)}$$ = 1389 kip/in (243.2 kN/mm), S_{td} = 10 ft. = 120 in. (3048 mm),

$$P_d = 13 t_d^{\ 1.894} L_d^{\ -0.541} \left(\frac{K_{td}}{S_{td}} \right)^{0.225}$$ = 126.2 kips (561 kN)

The predicted capacity using the alternative equation is 126.2 kips (561 kN) versus the predicted capacity using the modified STM [141.3 kips (629 kN)].

CONCLUSIONS

The following conclusions may be made based on the development process of a new analysis tool for the reinforcement free-decks:

1 The design load for reinforcement-free bridge decks on concrete wide flange girders was examined based on the current AASHTO specification and previous studies on the capacity of concrete decks under moving vehicle loads. The controlling state is the fatigue limit state requiring a strength design load of 97 kips (431 kN) for a vehicle wheel load. This is a much more severe design load than used in present design methods and specifications, but the capacities of the restrained deck are also higher than expected.

2 The proposed equivalent 2D strut-and-tie model (STM) can effectively replace a time consuming FEM analysis for predicting the capacity of a 7 in. (178 mm) or thicker [to 12 in. (305mm)] restrained deck on concrete wide flange girders when the deck clear span does not exceed 5 ft. (1524 mm) if the parameters predefined in **Tables 1-4** are used. This limitation does not hinder the practical application of the modified STM for the reinforcement-free deck system since the minimum thickness of the deck prescribed in AASHTO LRFD bridge design specification[15] is 7 in. (178 mm) and the clear deck span of concrete wide flange girder bridges rarely exceeds 5 ft. (1524 mm).

3. The model is capable of capturing the punching shear failure and the failure at mid-span due to flexural crushing of concrete. The model provides an acceptable 2D axisymmetric representation of the behavior of the restrained 3D deck.
4. The predicted capacities using the STM analyses for a 7.5 in. (191 mm) deep deck are acceptable when the clear deck spans were between 3 ft. and 5 ft. (914 mm and 1524 mm). When the clear deck span was 6 ft. (1829 mm) the STM analysis showed 4 ~ 18% higher capacity compared to the FEM analysis. This result indicates that the proposed method should currently be limited to deck clear spans of 5 ft. (1524 mm) or less.
5. The proposed method may be used for steel girders with clear deck spacing of less than 5 ft. (1524 mm). In order to apply the method to steel girders it is necessary to evaluate the contribution of the steel girders to the lateral stiffness of the restraining system.

ACKNOWLEDGEMENT

This project was supported through funding provided by the Federal Highway Administration through the Wisconsin Department of Transportation under the Innovative Bridge Research and Construction program.

NOTATION

a = height of a Whitney equivalent rectangular compressive stress block

A_{ds} = average cross-sectional area of the diagonal strut

A_t = cross-sectional area of a single steel tension tie

b = lateral (in perpendicular direction to the girder) length of the rectangular loading area

d = longitudinal (in parallel direction to the girder) length of the rectangular loading area

D = diameter of equivalent circular loading area

E_g = elastic modulus of the girder

E_s = modulus of elasticity of steel

f_{ct} = tensile strength of the deck given by $5\sqrt{f_c'}$ psi ($0.415\sqrt{f_c'}$ MPa), $\sqrt{f_c'}$ in psi (MPa)

I_{yg} = weak axis moment of inertia of the girder

K_l = stiffness of the spring at the bottom left side of the 2D model

K_{lf} = lateral portion of the combined lateral stiffness

K_{lgb} = stiffness of the spring at the bottom left side of the 2D model due to weak axis bending of the girder

K_{lgt} = stiffness of the spring at the bottom left side of the 2D model due to torsion of the girder

K_{lm} = stiffness of the spring at the bottom left side of the 2D model

K_{lt} = stiffness of the spring at the bottom left side of the 2D model representing the lateral tension tie contribution to the restraint

K_{td} = axial stiffness of single lateral tie in Equation (25) [= $\frac{A_t E_s}{(S_g + t_w)}$, kips/in (kN/mm)]

K_{tt} = lateral stiffness of the tension ties resisting a single vehicle wheel

l_{ds} = length of the diagonal strut

L = deck clear span between girder flanges

L_d = deck clear span between girder flanges in Equation (25), in. (mm)

P_d = wheel load capacity of the deck in Equation (25), kips (kN)

P_l = a sum of radial outward thrust in the form of a single force in the 2D model

P_{usd} = capacity of the diagonal strut

P_{utls} = capacity of the lateral top strut

q = unit distributed thrust around the 3D cone

R = deck restraining factor

R_1 = a ratio of (cracked length found from FEM)/ l_{ds}

S_t = spacing of the tension ties

S_{td} = spacing of the tension ties in Equation (25), in. (mm)

S_g = center to center spacing of the girders

S_w = spacing of the vehicle axle in a longitudinal (parallel direction to the girder) direction

t = deck thickness

t_d = deck thickness in Equation (25), in. (mm)

t_w = thickness of the web of the girder

T = sum of tensile force in the ties

T_r = sum of resisting capacity of the ties

w_{avg12} = average width of w_1 and w_2

w_{ds} = width of diagonal strut around half the circumference of the failure cone, in r direction

w_1 = width of the diagonal strut at its bottom

w_2 = width of the diagonal strut at its top

β_1 = a factor relating the depth of equivalent rectangular compressive stress block to the neutral axis depth

δ_l = lateral displacement in the STM due to the elongation of the restraints

δ_{lgb} = lateral displacement due to bending of the girder in its weak axis

δ_{lgt} = lateral torsional displacement at the top of the girder

δ_{lt} = lateral displacement in STM due to the elongation of the tie

δ_1 = lateral displacement at the loading location

δ_2 = lateral displacement at the shear center of the girder

ε_{vr} = strain in the virtual reinforcement

θ_1 = angle of inclination of the diagonal strut

θ_2 = spreading angle of the compressive force

REFERENCES

1. Schlaich, J.; Schafer, K.; and Jennewein, M., “Towards a Consistent Design of Structural Concrete,” *Journal of the Prestressed Concrete Institute*, V. 32, 1978, pp. 74-150.

2. ACI Committee 318, “Building Code Requirements for Structural Concrete (ACI 318-08) and Commentary (318R-08),” American Concrete Institute, Farmington Hills, MI, USA, 2008.

3. Tan, K. H., “Size Effect on Shear Strength of Deep Beams: Investigating with Strut-and-Tie Model,” *Journal of the Structural Engineering*, ASCE, V. 132, No. 5, 2006, pp. 673-685.

4. Brena, S. F., and Morrison, M. C., “Factors Affecting Strength of Elements Designed using Strut-and-Tie Models,” *ACI Structural Journal*, V.104, No. 3, 2007, pp. 267-277.

5. Ley, M. T.; Riding, K. A.; Widianto.; Bae, S.; and Breen, J. E., “Experimental Verification of Strut-and-Tie Model Design Method,” *ACI Structural Journal*, V. 104, No. 6, 2007, pp. 749-755.

6. Park, J., and Kuchma, D., “Strut-and-tie Model Analysis for Strength Prediction of Deep Beams,” *ACI Structural Journal*, V. 104, No. 6, 2007, pp. 657-666.

7. Hewitt, B. E,. and Batchelor, B. deV., “Punching Shear Strength of Restrained Slabs,” *Journal of Structural Division*, ASCE, V. 101, No. ST9, 1975, pp. 1837-1853.

8. Kuang, J. S., and Moley, C. T., “A Plasticity Model for Punching Shear of Laterally Restrained Slabs with Compressive Membrane Action,” *International Journal of Mechanical Sciences*, V. 32, No. 5, 1993, pp. 371-385.

9. Mufti, A. A., and Newhook, J. P., “Punching Shear Strength of Restrained Concrete Bridge Deck Slabs,” *ACI structural journal*, V. 95, No. 4, 1998, pp. 375-381.

10. Mufti, A. A.; Bakht, B.; and Jaeger, L. G., “Fiber FRC Deck Slabs with Diminished Steel Reinforcement,” *IABSE Symposium Proceedings (Leningrad)*, 1991, pp. 388-389.

11. Mufti, A. A.; Jaeger, L. G..; Bakht, B.; and Wegner, L. D., “Experimental Investigation of Fibre-reinforced Concrete Deck Slabs without Internal Steel Reinforcement,” *Canadian Journal of Civil Engineering*, V. 20, No. 3, Jun, 1993, pp. 398-406.

12. Oliva, M. G..; Bae, H.; Bank, L. C.; Russell, J. S.; Carter, J. W.; and Becker, S., “Design and Construction of a Reinforcement Free Concrete Bridge Deck on Precast Bulb Tee Girders,” *Proceedings 2007 PCI/FHWA National Bridge Conference*, Phoenix, AZ, USA, October 21-24, 2007, CD-ROM.

13. Naaman, A. E.; Wongtanakitcharoen; T.; and Hauser, G., “Influence of Different Fibers on Plastic Shrinkage Cracking of Concrete,” *ACI Materials Journal*, V. 102, No. 1, 2005, pp. 49-58.

14. Bae, H., “Design of Reinforcement-free Bridge Decks with Wide Flange Prestressed Precast Girders,” PhD Thesis, University of Wisconsin, Madison, WI, USA, 2008.

15. AASHTO., *AASHTO LRFD Bridge Design Specifications*, 4th Ed., American Association of State Highway and Transportation Officials, Washington, D.C., 2008.

16. Dieter, D. A.; Dietsche, J. S.; Bank, L. C.; Oliva, M. G.; and Russell, J. S., “Concrete Bridge Decks Constructed with FRP Stay-in-Place Forms and FRP Grid Reinforcing,” *Journal of the Transportation Research Board 1814*, TRB, National Research Council, Washington, D.C., 2002, pp. 219-226.

17. Bank, L. C.; Oliva, M. G.; Russell, J. S.; Jacobson, D. A., Conachen, M.; Nelson, B.; and McMonigal, D., “Double Layer Prefabricated FRP Grids for Rapid Bridge Deck Construction: Case Study,” *Journal of Composites for Construction*, ASCE, V. 10, No. 3, 2006, pp. 204-221.

18. Petrou, M. F.; Perdikaris, P. C.; and Wang, A., “Fatigue Behavior of Noncomposite Reinforced Concrete Bridge Deck Models,” *Transportation Research Board 1460*, TRB, National Research Council, Washington, D.C., 1994, pp. 73-80.

19. Hibbitt, Karlsson & Sorensen Inc., “ABAQUS User’s manual,” Hibbitt, Karlsson & Sorensen

Inc., Pawtucket, RI, USA, 2004.

20. Bae, H.; Oliva, M. G.; and Bank, L. C., "Obtaining optimal performance with reinforcement-free concrete highway bridge decks," *Engineering Structures*, V. 32, No. 8, 2010, pp. 2300-2309.

21. Wisconsin Department of Transportation., *WisDOT Bridge Manual*, Wisconsin Department of Transportation, Madison, WI, USA, 2010. (Website: http://www.dot.wisconsin.gov)

TABLES and FIGURES

List of Tables:

List of Figures:

Fig. 5 – Diagram of the lateral stiffness for the STM; (a) Plan view of the deck and girder; and (b) Components of lateral stiffness.

Fig. 6 – Diagrams to calculate the spring stiffness of the STM: (a) 3D model; and (b) 2D model.

Fig. 7 – Distribution of the lateral load acting on the girder.

Fig. 8 – FEM analysis of the girder to find the lateral displacement due to torsion of the girder: (a) Schematic drawing; and (b) Displacement at center span.

Fig. 9 – Stress and strain distribution in a mid-span section of the deck.

Fig. 10 – Simplification of the STM (E_d is modulus of elasticity of the deck).

Fig. 11 – Load vs. displacement plots from FEM analyses and restrained deck element experiment.

Fig. 12 – Ultimate capacity vs. deck restraining factor for 7.5 in. (191 mm) deep decks with 6 ft. (1829 mm) lateral tie spacing and: (a) Clear deck span = 3 ft. (914 mm); (b) Clear deck span = 4 ft. (1219 mm); (c) Clear deck span = 5 ft. (1524 mm); and (d) Clear deck span = 6 ft. (1829 mm).

Fig. 13 – Relationship between the predicted capacities of the deck using the alternative equation and those of the deck using 99 nonlinear FEM analyses.

Table 1–Ratio (R_2) for strut width found from nonlinear FEM analysis*

		Clear span of the deck, ft. (mm)			
		3 (914)	4 (1219)	5 (1524)	6 (1829)
Depth of the deck, in. (mm)	7.0 (178)	1.5	1.5	1.5	2.0
	7.5 (191)	1.5	1.5	1.5	2.0
	8.0 (203)	1.5	1.5	1.5	1.5
	8.5 (216)	1.5	1.5	1.5	1.5
	9.0 (229)	1.0	1.5	1.5	1.5

$* w_3 = R_2(w_1 + w_2)$

Table 2–Lateral torsional displacement [$\delta_{\lg t}$, in. (mm)] at the top of the girder found from FEM analyses under unit lateral load of 1 kip/in (0.177 kN/mm)

		Clear span of the deck, ft. (mm)			
		3 (914)	4 (1219)	5 (1524)	6 (1829)
Depth of the deck, in. (mm)	7.0 (178)	0.0155 (0.394)	0.0273 (0.693)	0.0339 (0.861)	0.0404 (1.026)
	7.5 (191)	0.0146 (0.371)	0.0257 (0.653)	0.0319 (0.810)	0.0380 (0.965)
	8.0 (203)	0.0137 (0.348)	0.0242 (0.615)	0.0304 (0.772)	0.0358 (0.909)
	8.5 (216)	0.0149 (0.378)	0.0228 (0.579)	0.0286 (0.726)	0.0337 (0.856)
	9.0 (229)	0.0152 (0.386)	0.0203 (0.516)	0.0256 (0.650)	0.0294 (0.747)

Table 3–Spreading angle (θ_2, degree) of the compressive force in diagonal direction found from nonlinear FEM analyses

		Clear span of the deck, ft. (mm)			
		3 (914)	4 (1219)	5 (1524)	6 (1829)
Depth of the deck, in. (mm)	7.0 (178)	55.89	54.49	48.93	25.46
	7.5 (191)	55.89	53.12	47.51	35.22
	8.0 (203)	47.55	43.66	40.21	30.62
	8.5 (216)	46.18	41.74	38.31	34.35
	9.0 (229)	43.66	43.47	41.74	44.51

Table 4–Ratio (R_1) of the cracked length over the length of the diagonal strut found from nonlinear FEM analyses

		Clear span of the deck, ft. (mm)			
		3 (914)	4 (1219)	5 (1524)	6 (1829)
Depth of the deck, in.	7.0 (178)	0.730	0.546	0.441	0.265
	7.5 (191)	0.733	0.565	0.438	0.270
	8.0 (203)	0.787	0.683	0.449	0.272
	8.5 (216)	0.802	0.719	0.444	0.337

(mm)	9.0 (229)	0.891	0.719	0.444	0.335

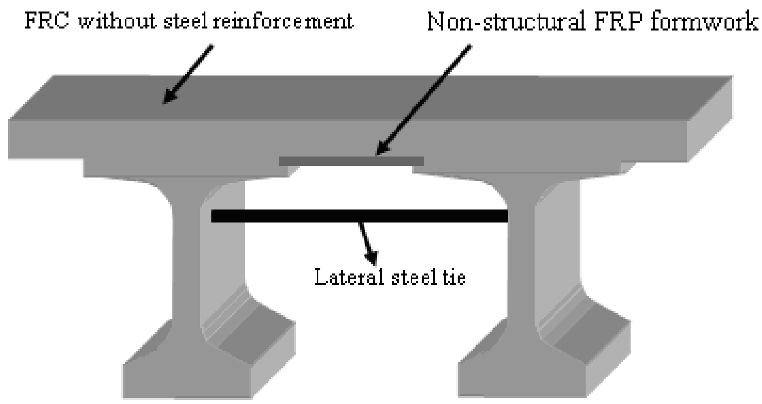

Fig. 1–Reinforcement-free deck concept.

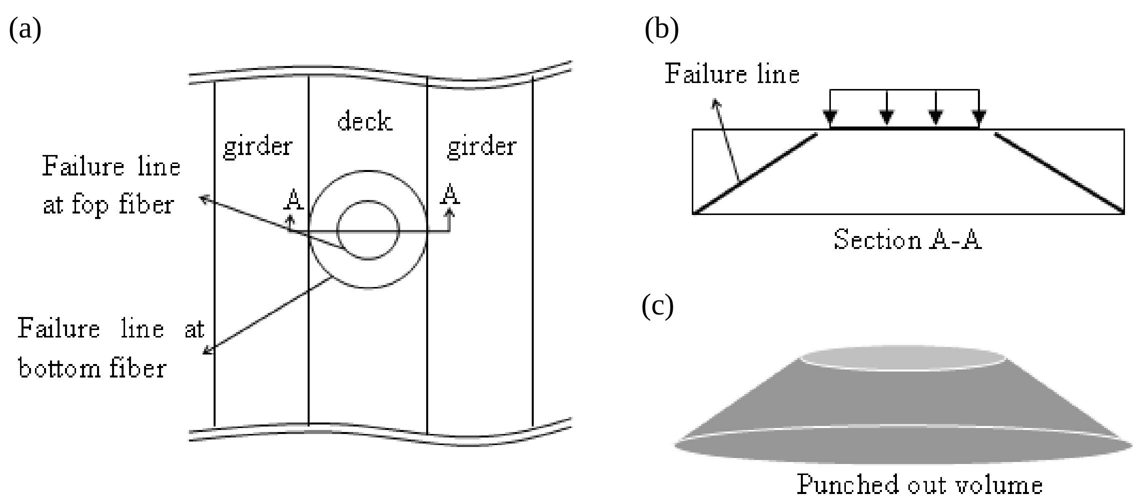

Fig. 2–Failure shape of the punching shear failure at the deck: (a) Plan view of the deck and girder; (b) Section A-A; and (c) Punched out volume.

(a) (b)

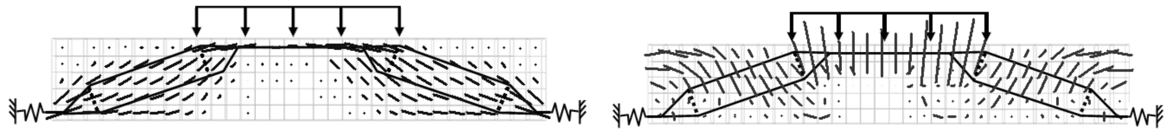

Fig. 3–Stress trajectory and STM of the deck: (a) Compressive stress trajectory; and (b) Tensile stress trajectory.

(a) (b)

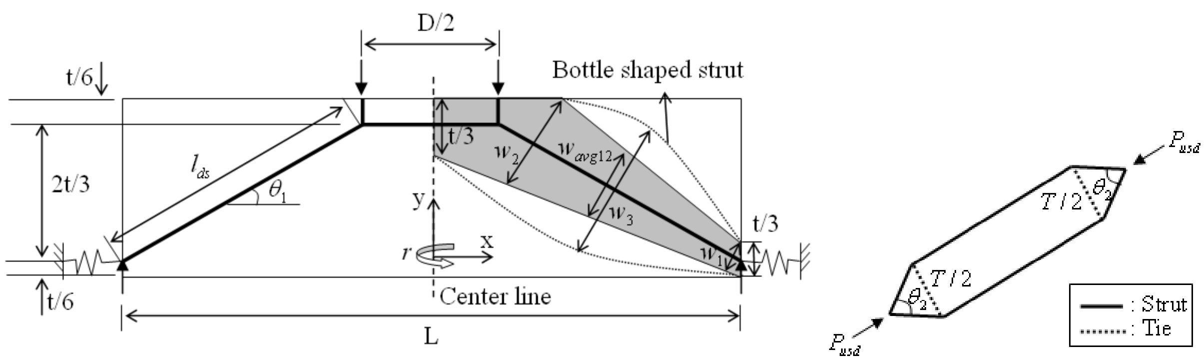

Fig. 4–Strut-and-tie-model: (a) Simplified STM and "bottle like" shape of the actual diagonal strut for the restrained deck with boundary condition; and (b) Detailed STM of diagonal strut.

(a) (b)

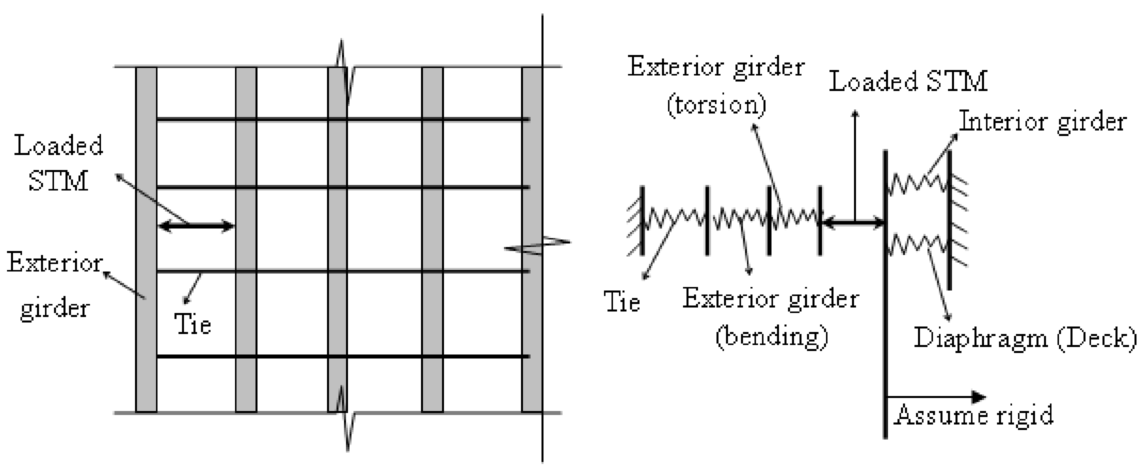

Fig. 5–Diagram of the lateral stiffness for the STM; (a) Plan view of the deck and girder; and (b) Components of lateral stiffness.

(a) (b)

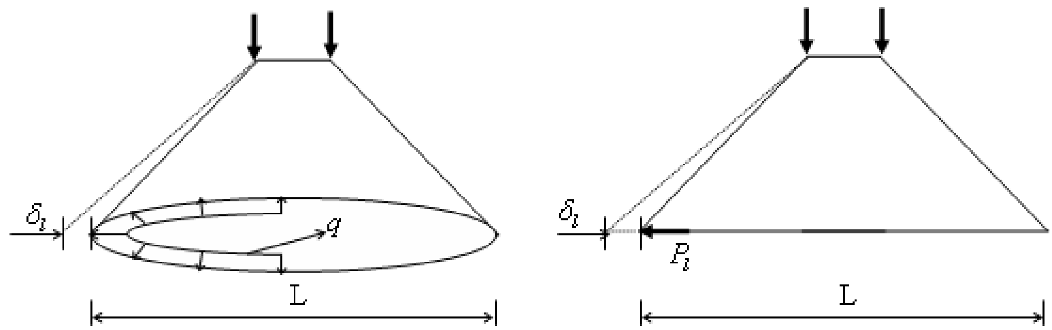

Fig. 6–Diagrams to calculate the spring stiffness of the STM: (a) 3D model; and (b) 2D model.

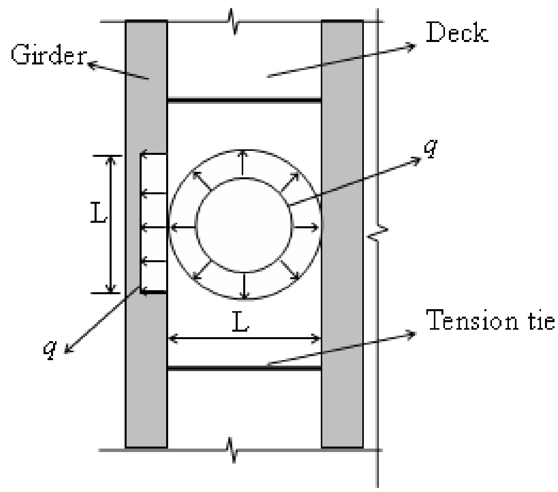

Fig. 7–Distribution of the lateral load acting on the girder.

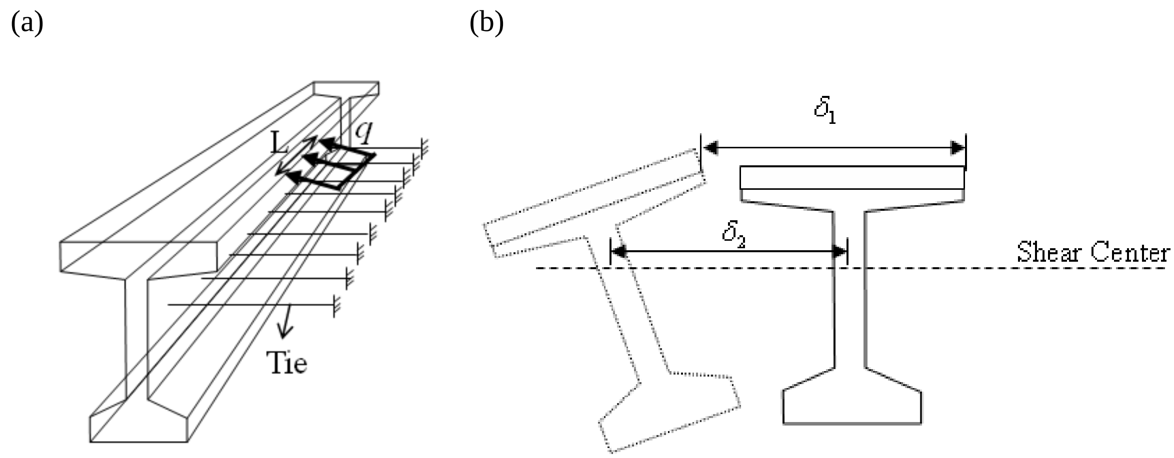

Fig. 8–FEM analysis of the girder to find the lateral displacement due to torsion of the girder: (a) Schematic drawing; and (b) Displacement at center span.

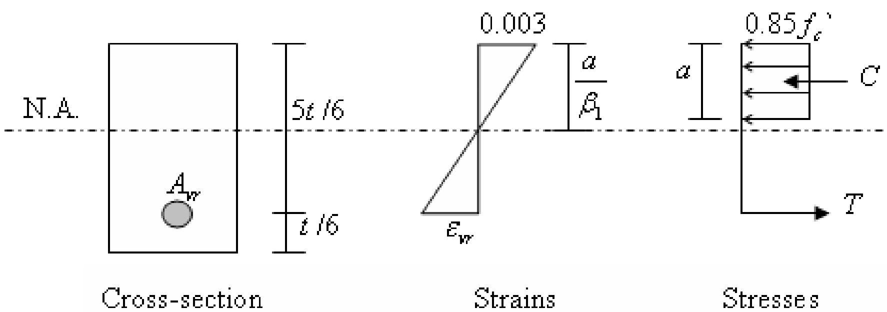

Fig. 9–Stress and strain distribution in a mid-span section of the deck.

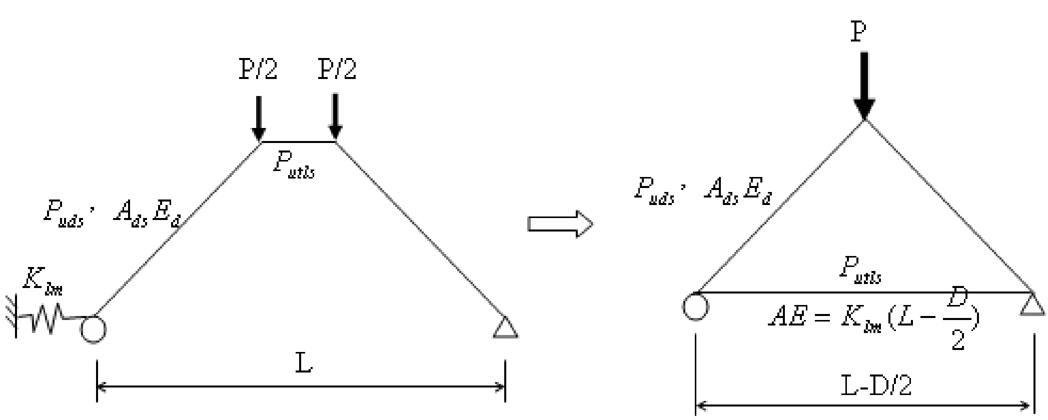

Fig. 10–Simplification of the STM (E_d is modulus of elasticity of the deck).

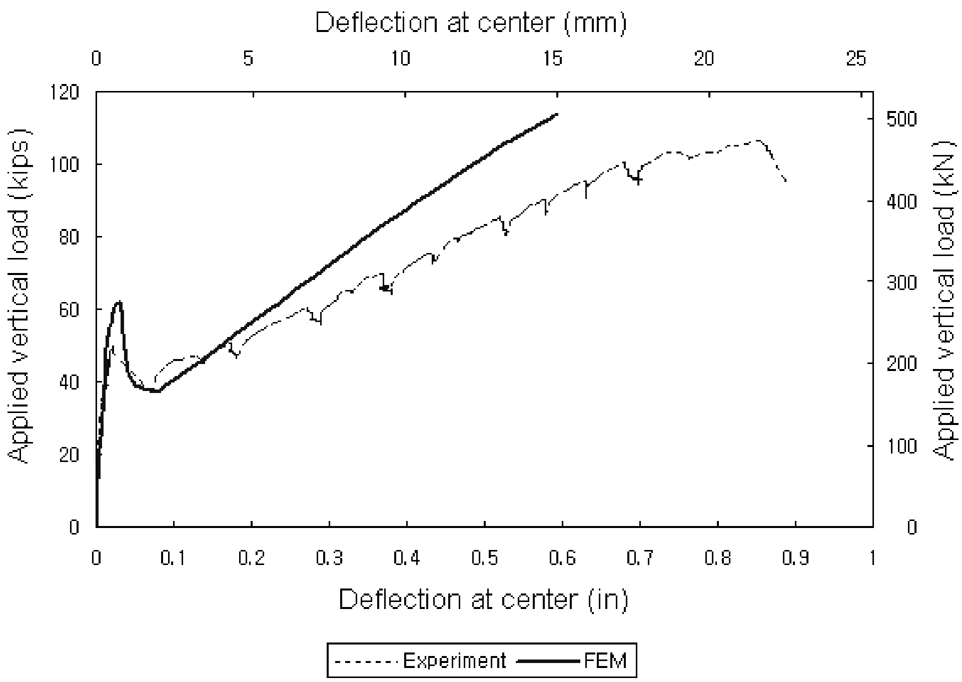

Fig. 11– Load vs. displacement plots from FEM analyses and restrained deck element experiment.

(a)

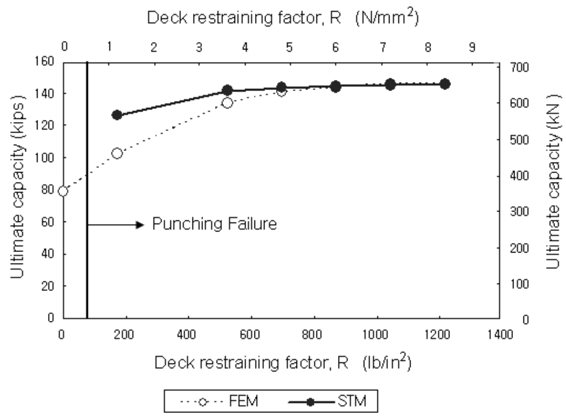

(b)

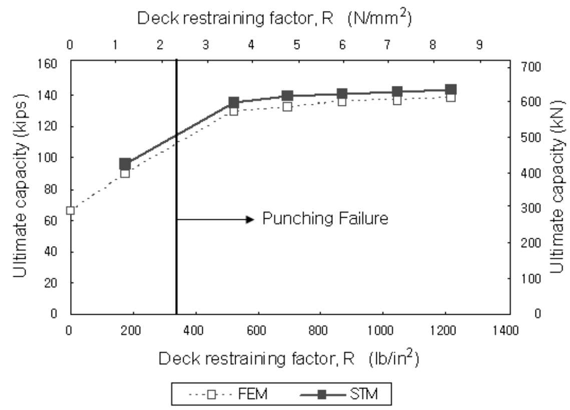

(c)

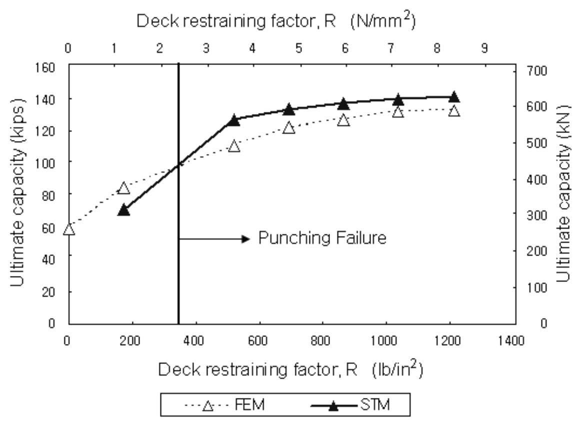

(d)

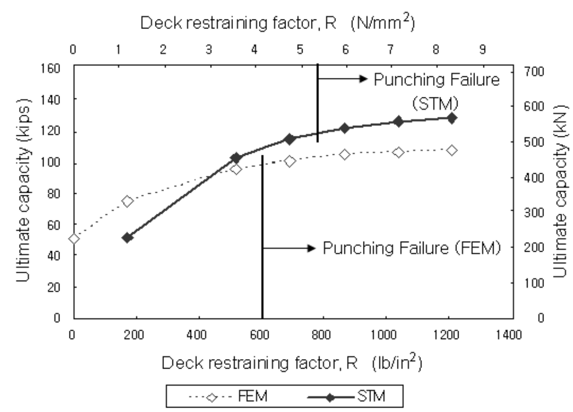

Fig. 12–Ultimate capacity vs. deck restraining factor for 7.5 in. (191 mm) deep decks with 6 ft. (1829 mm) lateral tie spacing and: (a) Clear deck span = 3 ft. (914 mm); (b) Clear deck span = 4 ft. (1219 mm); (c) Clear deck span = 5 ft. (1524 mm); and (d) Clear deck span = 6 ft. (1829 mm).

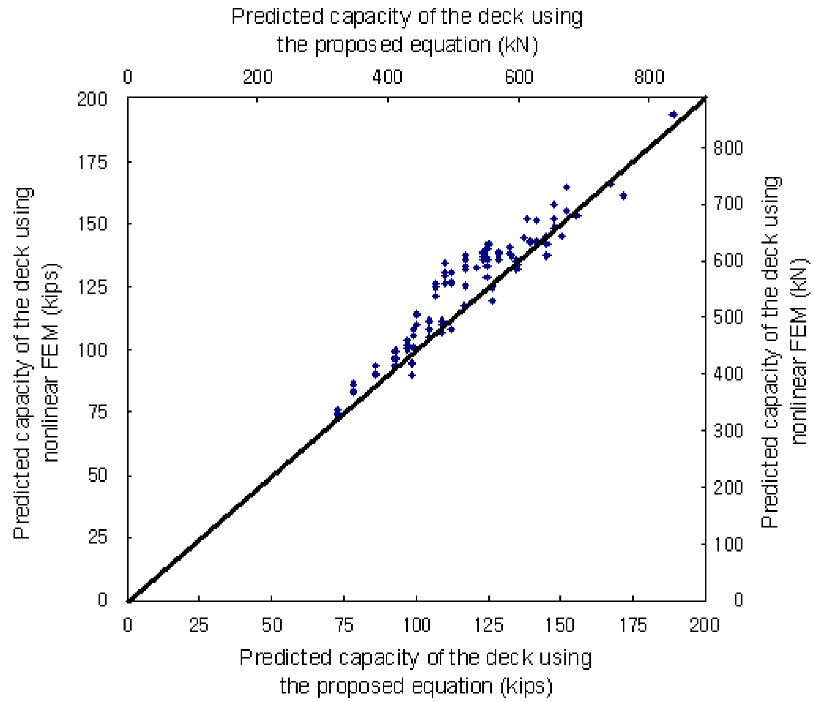

Fig. 13–Relationship between the predicted capacities of the deck using the alternative equation and those of the deck using 99 nonlinear FEM analyses.